Quantifying the toxicity of mixtures of metals and metal-based nanoparticles to higher plants

Liu, Y.

Chapter 5

Evaluating the combined toxicity of Cu and ZnO nanoparticles: utility of the concept of additivity and a nested experimental design.

Yang Liu, Jan Baas, Willie J.G.M. Peijnenburg,

Martina G. Vijver

Submitted

Abstract

We evaluated the combined toxicity of Cu and ZnO nanoparticles (NPs) using six nested combinations, $Cu(NO_3)_2$- $Zn(NO_3)_2$, $Cu(NO_3)_2$-CuNPs, $Zn(NO_3)_2$-ZnONPs, $Cu(NO_3)_2$-ZnONPs, $Zn(NO_3)_2$-CuNPs, CuNPs-ZnONPs. Each type of metal-based NPs was presumed to be a mixture containing soluble metal species and undissolved solid metal particles. A $Zn(NO_3)_2$ or $Cu(NO_3)_2$ solution was used as a reference to assess the toxicity of the dissolved fraction of ZnO NPs or Cu NPs. Effect measurements were performed using root elongation of *Lactuca sativa* L. Results were interpreted with the independent action (IA) model. This showed a good predictive power in estimating mixture toxicity of $Zn(NO_3)_2$-ZnONPs (R^2=0.84), $Cu(NO_3)_2$-CuNPs (R^2=0.94) and CuNPs-ZnONPs (R^2=0.82). The variations left in toxicity modeling of $Zn(NO_3)_2$-ZnONPs mixtures were explained by small antagonistic effects found between particulate ZnO and dissolved Zn which were not observed for $Cu(NO_3)_2$-CuNPs mixtures. Besides antagonistic effects between dissolved Cu and Zn, statistically significant relationships were also observed between increased concentrations of particulate Cu or Zn and increased median effective concentrations of $Zn(NO_3)_2$ or $Cu(NO_3)_2$. Results illustrated that 'interaction' between dissolved and particulate fractions of metal-based NPs affected the combined toxicity of Cu NPs and ZnO NPs, which complicated their observed effects as compared to mixtures of Cu and Zn nitrates.

Keywords: Cu; Zn; nanoparticles; mixture; toxicity

5.1 Introduction

Nanotechnology has been applied to create novel materials with unique characteristics in a large variety of consumer and household products. For example, engineered zinc oxide nanoparticles (NPs) are added into personal care products and coatings, which benefits from their ability to efficiently absorb UV-light and their increased transparency to visible light (Rousk et al., 2012). Nano-Cu powders can be dispersed into catalysts, conductive pastes, sintering additives, anti-bacteria products, and lubricant additives owing to their potential catalytic, dielectric, and biomedical properties (Mortimer et al., 2010). Increasing numbers of applications

may lead to direct or indirect releases of engineered metal-based NPs into the environmental. This may pose effects on a variety of organisms in aquatic and terrestrial eco-systems, and in turn requires more attention on their eco-toxicological effects.

Dissolution and aggregation/agglomeration are the two main processes that can strongly influence the state of metal-based NPs present in suspensions, and consequently impact the bioavailability, uptake and toxicity of NPs (Misra et al., 2012). It has been reported that various characteristics of the exposure media can affect dissolution and aggregation of metal-based NPs, e.g. pH, ionic strength and the presence of naturally occurring organic matter (Franklin et al., 2007). Dissolution of NPs is a dynamic process in which constituent molecules of the dissolving solid migrate from the surface to the bulk solution through a diffusion layer (Borm et al., 2006). The adsorption of molecules and ions from solution can promote or delay the dissolution process by modifying the diffusion layer characteristics (Adamson and Gast, 1997). Apart from heteroaggregation, particles can also be bound together (homoaggregation) when their equilibrium solubility is above saturation concentrations (Holsapple et al., 2005), which can increase the overall diffusion layer thickness and hinder dissolution of NPs.

Metal-based NPs are always an intermediate state of bulk and molecular materials. Metal ions or small inorganic complexes produced by engineered metal-based NPs consisting of highly toxic elements inevitably drive the partial toxicity of metal-based NPs to organisms (Misra et al., 2012). However, it is still a challenge to clarify which metal species contribute most to the nano-toxicity. Some studies suggested that the toxic effects of ZnO NPs and Cu NPs on environmentally relevant organisms were most likely due to the dissolved metal species rather than being particle-dependent (Blinova et al., 2010; Bondarenko et al., 2012; Ivask et al., 2013). Other researchers argued that the particulate forms of ZnO NPs and Cu NPs contributed substantially to the cytotoxic effects on mammalian and piscine cell lines (Fernández-Cruz et al., 2013; Song et al., 2014). The translation from an effect on a cell line to a whole organism is not straightforward and depends on numerous factors such as the types of cell lines and metal-based nanoparticles. Karlsson et al. (2014) found that the oxidative stress of mouse embryonic stem (mEs) cells was induced by the released

Cu ions of CuO NPs whereas the stress was particle related for NiO NPs.

Nano-ZnO has been classified as 'extremely toxic' to aquatic organisms, followed by 'very toxic' nano-Cu (Kahru and Dubourguier, 2010). They were already found to be simultaneously present in wastewater effluents (Bystrzejewska-Piotrowska et al., 2009; Bolyard et al., 2013; Li et al., 2015). These nanoparticles can enter the terrestrial system by the application of bio-solids from sewage systems as a fertilizer (Batley et al., 2012). Higher plants have been reported to be able to ingest and store metal-based NPs in tissues (Rico et al., 2011). To date, the knowledge of the eco-toxicity of Cu NPs and ZnO NPs is far from being adequate as compared to their large-scale application (Hu et al., 2010; Song et al., 2010), especially under conditions of their co-exposure.

This study aims at improving the understanding of effects of Cu NPs, ZnO NPs and their mixtures on *L. sativa* L. and unravelling two questions as follows: (1) Will the dissolved metals and the particulate metals of each type of metal-based NPs act jointly following the common rules of additivity? (2) Will Cu NPs interact with ZnO NPs and influence the toxicity of each other? Theoretically, if Cu NPs and ZnO NPs would act comparable to metal salts, e.g. $Cu(NO_3)_2$ and $Zn(NO_3)_2$, then the existing models for general eco-toxicology of metals such as the free ion activity model (FIAM) and the biotic ligand model (BLM) can be applied to predict the toxicity of metal-based NPs. As shown in our previous studies (Le et al., 2013; Liu et al., 2014), Cu^{2+} competed with Zn^{2+} for binding to the biotic ligand of lettuce. What makes this research more difficult than the case of mixtures of metal salts is that the suspensions of each type of metal-based NPs are a mixture mainly containing dissolved metal species and undissolved particles. Suspensions of Cu NPs and ZnO NPs were therefore assumed to contain four metal species i.e. dissolved Cu, dissolved Zn, particulate Cu and particulate ZnO. Cedergreen et al. (2012) have shown that the joint effect of ternary mixtures can be predicted from binary mixture toxicity results. To trace down the potential 'interactions' between Cu NPs and ZnO NPs and where these 'interactions' (if any) take place, an elaborate nested experiment was designed including all possible combinations:

- $Cu(NO_3)_2$- $Zn(NO_3)_2$ (dissolved Cu and dissolved Zn, Cu-Zn)

- $Cu(NO_3)_2$ and Cu NPs (dissolved Cu and particulate Cu, Cu-nanoCu)
- $Zn(NO_3)_2$ and ZnO NPs (dissolved Zn and particulate ZnO, Zn-nanoZnO)
- $Zn(NO_3)_2$ and Cu NPs (dissolved Zn and particulate Cu, Zn-nanoCu)
- $Cu(NO_3)_2$ and ZnO NPs (dissolved Cu and particulate ZnO, Cu-nanoZnO)
- Cu NPs and ZnO NPs (particulate Cu and particulate ZnO, nanoCu-nanoZnO)

A $Zn(NO_3)_2$ or $Cu(NO_3)_2$ solution was used as a reference to assess the single toxicity of the dissolved fraction of ZnO NPs or Cu NPs. The combined effects caused by nanoCu-nanoZnO mixtures were then compared with the overall effects of $Cu(NO_3)_2$ and $Zn(NO_3)_2$ the data of which have been reported in the study of Le et al. (2013).

5.2 Methods

5.2.1 Test compounds and nutrient solution

The engineered uncoated Cu NPs (nano-spheres, nominal particle size 50 nm, NM-0014, purity 99.8%) and the engineered uncoated ZnO NPs (nano-sticks, nominal particle size 150 nm, NM-110) were purchased from the io-li-tec company (Heilbronn, Germany). $Cu(NO_3)_2 \cdot 3H_2O$ (purity 99.5%), $Zn(NO_3)_2 \cdot 6H_2O$ (purity 99.5%) and other salts used in preparing the nutrient solution were all purchased from the Merck KGaA company (Darmstadt, Germany). The nutrient solution was composed of $Ca(NO_3)_2 \cdot 4H_2O$ (236.1 mg/L), $MgSO_4 \cdot 7H_2O$ (60 mg/L), $NaHCO_3$ (50 mg/L), and $KHCO_3$ (10 mg/L) totally dissolved in demi-water (pH 7.8) and was applied for culturing plants and preparing exposure medium.

5.2.2 Experimental design

A full factorial experimental design included all the six possible combinations of particles and dissolved metal species. A detailed description of the experimental setup after pre-screening tests is represented in Figure S5.1. Negative controls (nutrient solution) and positive controls (single compounds, i.e. $Cu(NO_3)_2$, $Zn(NO_3)_2$, Cu NPs, ZnO NPs individually) were both conducted every week with mixture treatments and were repeated twice. Hydroponic exposure was used to avoid complex interactions of particles and ions in the soil compartment. To keep the concentrations of compounds in solution constant, the test media were replaced

every day. Stock suspensions of Cu NPs and ZnO NPs were daily prepared in nutrient solution and sonicated in an S 40 H Elmasonic water bath sonicator (Elma, Germany) for 10 min. All the stock solutions including the nitrate salts were further diluted 10 times with nutrient solution to obtain the nominal concentrations for each treatment.

5.2.3 Exposure of lettuce and toxicity determination

Lactuca sativa L. was selected as the test organism because this species can be manipulated relatively easily and it is sensitive to environmental contaminants (OECD, 2006). The toxicity tests were operated according to guidelines of the US Environmental Protection Agency (EPA, 1988). As compared to the germination rate of seeds, the relative root elongation rate (*RRE*, %) of lettuce seedlings was more realistic in reflecting external stressors (Pfleeger et al., 1991) and therefore was employed as the toxicological endpoint in this study. Lettuce seeds were purchased from the Horti Tops company (Amsterdam, the Netherlands) and germinated on expanded perlite in a climate room (18°C, 80% humidity, and a 16:8 h light: dark cycle) for 96 h. After germination, seedlings with taproot lengths more than 3 cm were chosen to be fixed on parafilm strips floating on the surface of glass petri dishes containing 30 ml test medium. In each petri dish, 4 seedlings were suspended. Before and after 96 h exposure, the length of lettuce taproot was measured from the transition point between the hypocotyls and the root to the root tip. The root growth of each treatment was defined as the mean value of differences in root length of 4 seedlings before and after exposure. Then *RRE* was determined as follows

$$RRE = \frac{RG_S}{RG_C} \times 100\% \quad (5\text{-}1)$$

where RG_s: the root growth of plants in the sample solution, cm; RG_c: the root growth of plants in the control solution, cm.

5.2.4 Characterization of nanoparticles

The morphology and particle size of metal-based NPs were characterized using a JEOL 1010 Transmission Electron Microscope (JEOL, Japan). The particle size of Cu NPs and ZnO NPs was analyzed using a Nano Measurer 1.2 (Fudan University,

China). The distribution of the hydrodynamic diameter and the zeta-potential of NPs in different spiked test media were measured after 1 h and 24 h of preparation by Dynamic Light Scattering (DLS) on a Zetasizer Nano-ZS instrument (Malvern, United Kingdom).

5.2.5 Chemical analysis

A Cu-ion selective electrode (Cu-ISE, Metrohm, Switzerland) was used as a direct way to measure the free Cu-ion activity in solution after 1 h and 24 h. The Zn-ion selective electrode was not used in this study because the detection limit was not sufficient for the test. To check whether particles will reduce the sensitivity of the Cu-electrode membrane, plain polystyrene fluorescent microspheres # 103125-05 (nominal particle size 70 nm, Microspheres-Nanospheres, American) were added to compare the activities of Cu^{2+} with those in solutions of $Cu(NO_3)_2$ alone. The actual total concentrations of Ca, Mg, Na, K, Cu, Zn, and the dissolved concentrations of Cu and ZnO NPs after 1 h and 24 h of equilibration were analyzed using Flame Atomic Absorption Spectroscopy (Perkin Elmer AAnalyst 100, American). Centrifugation of samples removed Cu NPs, ZnO NPs and ions which may be adsorbed to particle surfaces. The supernatants were obtained after 20 min of centrifugation in a Centrifuge 5415D (Eppendorf, Germany) at 13 300 *g* (Fernández-Cruz et al., 2013). The particle suspensions, the supernatants and the liquids with nitrate salts were digested using HNO_3 and sampled for FAAS analysis.

5.2.6 Data analysis

To check the potential chemical-chemical interactions before entering the organism, relationships between the free Cu^{2+} activities in the solution (or the dissolved metal species of Cu NPs or ZnO NPs) and the added amount of one compound in mixtures of Cu-nanoCu, Zn-nanoZnO, Cu-nanoZnO, Zn-nanoCu, and nanoCu-nanoZnO after 1 h and 24 h of exposure were all analyzed using the linear regression method in the GraphPad Prism 5 software (GraphPad, American). For the Cu-nanoCu mixtures, the activities of Cu^{2+} released from Cu NPs were calculated by subtracting the Cu^{2+} activities of $Cu(NO_3)_2$ from the totally measured activities of Cu^{2+} in mixture solutions. The actually total or dissolved concentrations of Cu NPs or ZnO NPs in Cu-nanoCu and Zn-nanoZnO mixtures were calculated in a similar way.

To check the potential interactions after compounds entered the organism, the independent action (IA) model based on the rules of 'additivity' (Bliss, 1939) was initially used to predict the combined toxicity of mixtures of Cu-nanoCu, Zn-nanoZnO and nanoCu-nanoZnO since the effect of each compound in a mixture can be directly measured from positive controls.

$$E(C_{\text{mix}}) = 1 - \prod_{i=1}^{n} [1 - E(C_i)] \quad (5\text{-}2)$$

where $E(C_{\text{mix}})$: the estimated effect of an n-compound mixture; $E(C_i)$: the effect of the ith compound applied singly at a fixed concentration.

If compounds in a mixture do not act following the rules of 'additivity', 'interactions' between these compounds may play an important role in their combined toxicity. Finding interactions in mixtures is always a challenge especially when a mixture contains more than two components. Since the suspensions of Cu-nanoZnO, Zn-nanoCu, nanoCu-nanoZnO mixtures involve more than two metal species, searching interactions between these different metal species cannot be done using the existing models for binary mixtures. Therefore, a different approach was used in this study, which will be explained by the following example of Cu-nanoZnO mixtures.

To examine the influence of $Cu(NO_3)_2$ on the toxicity of ZnO NPs, the root growth inhibition caused by $Cu(NO_3)_2$ should be subtracted from the total effects of Cu-nanoZnO mixtures. The *RRE*s induced by ZnO NPs in co-exposure of $Cu(NO_3)_2$ and ZnO NPs can be calculated by substituting the RG_c of positive controls (with $Cu(NO_3)_2$ alone) in equation (1). The *RRE*s induced by ZnO NPs alone can be calculated by substituting the RG_c of negative controls (nutrient solution only) in equation (5-1). The median effective concentrations (EC_{50}s) of ZnO NPs in single-exposure or co-exposure with $Cu(NO_3)_2$ were all calculated using the log-logit function in GraphPad Prism 5. The EC_{50} values of ZnO NPs in the co-exposure with $Cu(NO_3)_2$ were then compared with the EC_{50} value of ZnO NPs in single exposure. It was assumed that if the EC_{50}s of ZnO NPs in the co-exposure with $Cu(NO_3)_2$ were significantly different from the value of ZnO NPs in single exposure, then the influence of $Cu(NO_3)$ on the toxicity of ZnO NPs was statistically significant. The EC_{50} values of ZnO NPs were plotted as a function of increasing concentrations of

$Cu(NO_3)_2$ by the linear regression in OriginPro 8 (Origin Lab, United Kingdom). As an initial attempt, the slope of straight lines was compared with zero to indicate the overall antagonism or synergism. A non-significant slope is indicative of no substantial effects of $Cu(NO_3)_2$ on the toxicity of ZnO NPs, a significant positive ($p < 0.05$) slope is indicative of antagonistic effects, and a significant negative slope indicates synergistic effects. Similar methods can be used to find out the influence of ZnO NPs (in both dissolved and particulate forms) on the toxicity of $Cu(NO_3)_2$ and for other mixtures investigated in this study.

To determine whether Cu NPs and ZnO NPs have similar effects as $Cu(NO_3)_2$ and $Zn(NO_3)_2$, the biological responses (*RRE*, %) caused by mixtures of nanoCu-nanoZnO and of Cu^{2+}-Zn^{2+} were plotted as the 2D isobolic representations by the software of OriginPro 8. Data for the toxicity of Cu^{2+} and Zn^{2+} to *L. sativa* L. were obtained under similar environmental environment, and are published by Le et al. (2013). The x-axis or y-axis was presented as toxic unit (TU) for each compound (1TU=the median effective concentration). The theoretical line of additivity is the straight line that connects the individual doses of each compound in a mixture to produce a fixed equal effect alone. In general terms, isoboles represent an upward curve (round) when the combined effects are less than addition and isoboles become hollow when mixture effects are more toxic than addition (Bongers, 2007).

5.3 Results

5.3.1 Characterization of nanoparticles

The TEM images of Cu NPs, ZnO NPs and their mixtures are shown in Figure 5.1. The primary sizes and shapes of the particles were estimated based on the TEM images. The Cu NPs were shown to be of spherical shape, 127 nm in size (size variation of 119-137 nm). The ZnO NPs crystals were approximatively displayed tetragonal morphology (width: 55 nm, size variation of 24-110 nm; length: 144 nm, size variation of 95-224 nm). The size distribution of the hydrodynamic diameter of NPs in lettuce culture solution and in solution of five combinations was determined using DLS and shown in Table S5.1. Initial particle sizes changed quickly after the NPs were submerged in lettuce culture solution. Both NPs were present as aggregates (370 nm - 1531 nm) in lettuce culture solution and in mixture solutions.

The hydrodynamic particle sizes of Cu NPs and ZnO NPs increased by a factor of 1.5 to 2 after 24 h submerged in lettuce culture solution and in solution of mixtures of Zn-nanoCu, nanoCu-nanoZnO, Zn-nanoZnO. Besides, the absolute values of zeta-potential of NPs were < 14 mV. This indicated that the suspensions of NPs were relatively less stable which resulted in the aggregates by Van Der Waals inter-particle force.

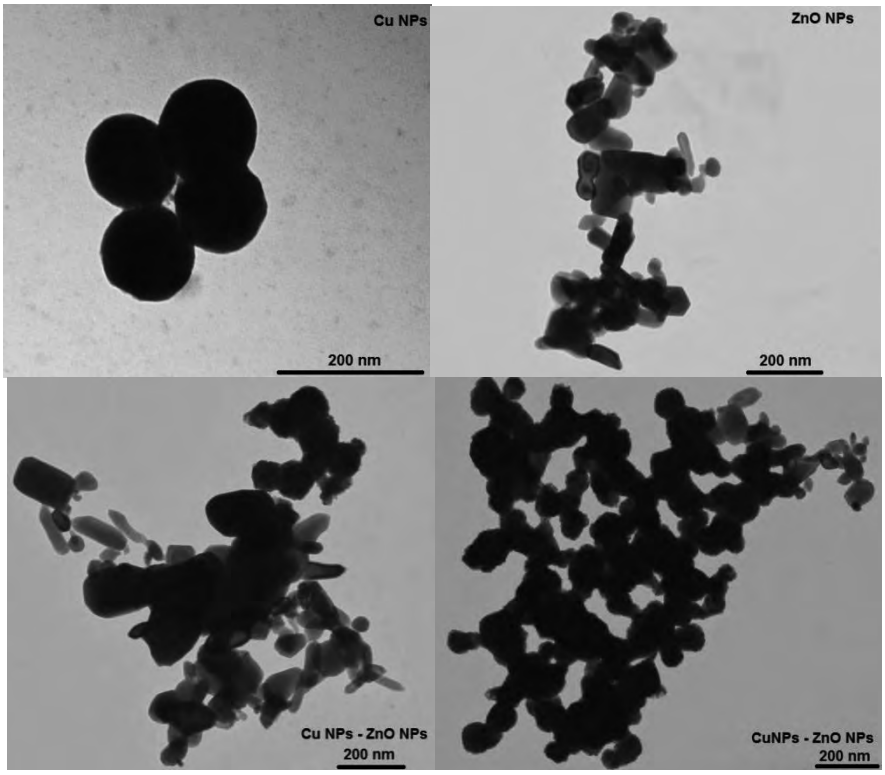

Figure 5.1 The TEM images of Cu NPs, ZnO NPs and their mixtures. Scale bars indicate size (nm).

5.3.2 Fate analysis

Relationships between the free activities of Cu^{2+} in solution and the added ZnO NPs, $Zn(NO_3)_2$, Cu NPs, $Cu(NO_3)_2$ after 1 h and 24 h are plotted in Figure S5.2. After 24 h, the activities of Cu^{2+} were generally increased in mixtures of Cu-nanoCu, Zn-nanoCu, Cu-nanoZnO, and nanoCu-nanoZnO as compared to the values after 1 h. However, no consistently significant effects of increasing concentrations of

$Cu(NO_3)_2$, Cu NPs, $Zn(NO_3)_2$, ZnO NPs were observed on the activities of Cu^{2+} in solution after 1h and 24 h of equilibration using the Cu-ISE. This indicated that the amount of free Cu^{2+} released from either Cu NPs or $Cu(NO_3)_2$ was not substantially affected by other compounds of Cu or Zn added to the solution. It is shown in Figure S5.3 that the growing trend of Cu^{2+} activities in solution with polystyrene fluorescent microspheres remained constant when more $Cu(NO_3)_2$ was added and the slope of linear curves remained positive. This finding showed that polystyrene fluorescent microspheres did not reduce the sensitivity of Cu-ISE.

The background concentrations of Na, K, Ca, Mg in nutrient solution were respectively measured to be 11.9 ± 0.3 mg/L, 3.68 ± 0.07 mg/L, 31.24 ± 0.5 mg/L, 5.49 ± 0.08 mg/L. The impacts of addition of a compound to solution, on the dissolution of Cu NPs and ZnO NPs after 1h and 24 h of equilibration in mixtures of Cu-nanoCu, Zn-nanoZnO, Cu-nanoZnO, Zn-nanoCu, nanoCu-nanoZnO are represented in Figure S5.4. Generally, the more NPs were added to the solution, the lower proportion of dissolved fraction of the same type of metal-based NPs was measured after 1 h and 24 h. The dissolved concentrations of Cu NPs at the same dose levels were found to be higher after 24 h in all combinations which coincided with the increased values of free Cu^{2+} activities. No statistically significant impacts were observed from addition of $Zn(NO_3)_2$, $Cu(NO_3)_2$, and Cu NPs on the dissolution of ZnO NPs. Although the dissolved concentrations of Cu NPs at lower doses were significantly increased by the added $Cu(NO_3)_2$ after 1 h, the influence was not constant across the whole range of concentrations. Only for Zn-nanoCu mixtures, it was found that the dissolved concentrations of Cu NPs were significantly reduced by the added $Zn(NO_3)_2$ after 24 h.

5.3.3 Toxicity of individual compounds

Following the full factorial experimental design, a complete dose-response curve was obtained for each compound investigated in this study, which was used to calculate the EC_{50}s to *L. sativa* L. The averaged EC_{50} values of Cu NPs, ZnO NPs, $Cu(NO_3)_2$ and $Zn(NO_3)_2$ are provided in Table 5.1. Nano-ZnO had the minimum acute toxicity to lettuce as shown by its highest EC_{50} value and $Cu(NO_3)_2$ with the lowest EC_{50} resulted in the highest toxic effects on root growth. The EC_{50} values of nano-Cu and $Cu(NO_3)_2$ were similar, and the EC_{50} of nano-ZnO was twice as big as

for $Zn(NO_3)_2$.

Table 5.1 The median effective concentrations (EC_{50}, mg/L) with the 95% confidence interval (CI) of nano-Cu, nano-ZnO, $Cu(NO_3)_2$ and $Zn(NO_3)_2$ individually on root elongation of lettuce (*L. sativa* L.) in the present study.

Compounds	Forms	EC_{50} (mg/L)
Cu NPs	Total Cu	0.10 (0.08-0.11)
ZnO NPs	Total Zn	4.47 (3.39-5.85)
$Cu(NO_3)_2$	Dissolved Cu	0.07 (0.06-0.07)
$Zn(NO_3)_2$	Dissolved Zn	2.08 (1.75-2.39)

5.3.4 Toxicity of mixtures

In the present study, 82-94% of the variability in the toxicity of nanoCu-nanoZnO, Zn-nanoZnO and Cu-nanoCu mixtures could be explained by the independent action (IA) model (Figure 5.2). To examine whether potential 'interactions' were the cause of remaining deviations from the model, the effective concentrations causing a 50% reduction in root elongation of Cu NPs, ZnO NPs, $Cu(NO_3)_2$, $Zn(NO_3)_2$ in single-exposure and in co-exposure of Cu-nanoCu, Zn-nanoZnO, Cu-nanoZnO, Zn-nanoCu, and nanoCu-nanoZnO mixtures were plotted in Figure 5.3 as a function of the various dose levels of Cu or Zn in solution. The dissolved concentrations of metal-based NPs were expressed as the average values after 1 h and 24 h of equilibration. As shown in Figure 5.3 A-D, the EC_{50}s of nano-Cu were not statistically significantly increased with increasing concentrations of $Cu(NO_3)_2$ and significant impacts of Cu NPs were neither observed on the EC_{50}s of $Cu(NO_3)_2$. This implied that the dissolved Cu and the particulate Cu did not affect the toxicity of each other for lettuce (Table 5.2). For the combination of Cu-nanoZnO, the EC_{50}s of nano-Zn cannot be calculated in the second replicates when concentrations of $Cu(NO_3)_2$ were beyond 0.06 mg/L, which were thus not used in the data analysis. The EC_{50} of nano-Zn was still significantly increased, up to a factor of 5.5 at 0.05 mg/L of $Cu(NO_3)_2$. In Figure 5.3 F-H, the EC_{50} of $Cu(NO_3)_2$ at the highest concentration of ZnO NPs (42.2. mg/L) was not calculated due to the small

difference in root length as compared to the positive controls. Without this data point, the EC_{50} values of $Cu(NO_3)_2$ were significantly increased upon increasing amounts of ZnO NPs in the solution. For the combination of Zn-nanoCu, the EC_{50}s of $Zn(NO_3)_2$ were found to be sharply increased by the added Cu NPs regardless of the metal species in solution. However, a similar result was not observed in turn. The EC_{50} values of nano-ZnO significantly increased upon increasing concentrations of $Zn(NO_3)_2$ in solution. At lower concentrations of ZnO NPs, the EC_{50}s of $Zn(NO_3)_2$ were also increased with increasing concentrations of Zn NPs (b, N-P, Figure 5.3). This finding indicated that the dissolved Zn may compete against the particulate Zn for inducing toxicity to lettuce at lower concentrations of Zn NPs (< 20 mg/L). For the complex nanoCu-nanoZnO mixtures, the EC_{50}s of ZnO NPs cannot be calculated in the second replicates when concentrations of Cu NPs were higher than 0.05 mg/L and non-significant impacts of Cu NPs at lower concentrations were observed on the toxicity of ZnO NPs. The EC_{50}s of Cu NPs were observed to significantly increase with an increased amount of ZnO NPs in the solution (< 5mg/L).

The biological responses caused by mixtures of nanoCu-nanoZnO and mixtures of Cu^{2+}-Zn^{2+} are plotted in Figure 5.4. For the combination of Cu^{2+}-Zn^{2+}, the toxicity was dominated by Cu^{2+} at lower concentrations of Zn^{2+} and antagonistic effects occurred. At higher concentrations of Zn^{2+}, the toxicity was relatively dominated by Zn^{2+} and synergistic effects occurred. A similar dose ratio-dependent deviation pattern was not observed for the combination of nanoCu-nanoZnO. Antagonism is observed at lower effect levels, whereas deviation patterns were found to be dependent on the concentration ratios of Cu NPs and ZnO NPs at high effect levels. Synergistic effects occurred if the combined toxicity was dominated by Cu NPs and a mixture acted antagonistic if ZnO NPs relatively dominated.

5.4 Discussion

5.4.1 Fate of nanoparticles

The size of Cu NPs and ZnO NPs in culture media of lettuce was not observed to be strongly affected by the added amount of $Cu(NO_3)_2$ and $Zn(NO_3)_2$ in solution after 1 h and 24 h of equilibration. This may be attributed to the high tendency of both NPs

to aggregate after submersion in nutrient solution. The high concentrations of ingredients in nutrient solution can be a reason for rapid and dramatic aggregation (Franklin et al., 2007). The increasing concentrations of Cu or Zn in the exposure media were shown not to hinder or stimulate the dissolution of Cu NPs or ZnO NPs and therefore the ion release of Cu NPs except in the co-exposure of $Zn(NO_3)_2$ and Cu NPs after 24 h. This may be caused by incompletely separating the dissolved metal species from nanoparticles, since there is still no definitely effective technique for assessing dissolution of bulk materials to NPs (Misra et al., 2012). Alternatively, unlike the other properties of water chemistry such as pH, HPO_4^{2-} and DOM (Li et al., 2013), the dissolved Cu and Zn in solution cannot strongly influence the dissolution of Cu NPs and ZnO NPs.

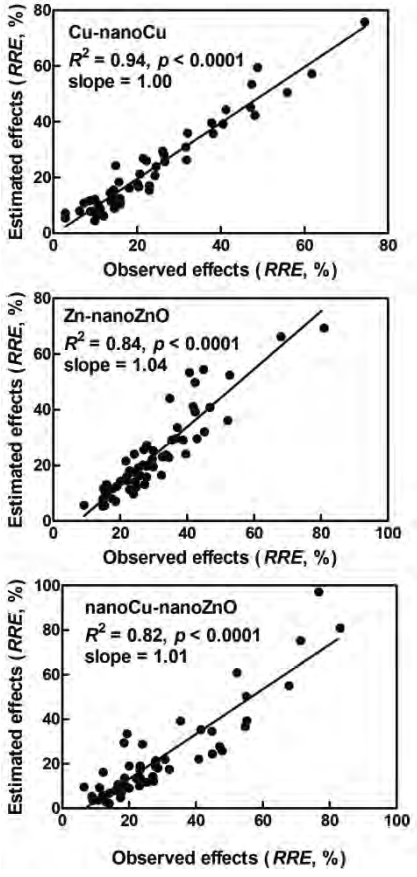

Figure 5.2 Relationships between the estimated and the observed effects of mixtures of Cu-nanoCu, Zn-nanoZnO and nanoCu-nanoZnO on relative root

elongation (*RRE*, %) of lettuce *Lactuca sativa* L. using the independent action (IA) model. R^2 indicates the determination coefficient. *p* indicates the statistical significance level.

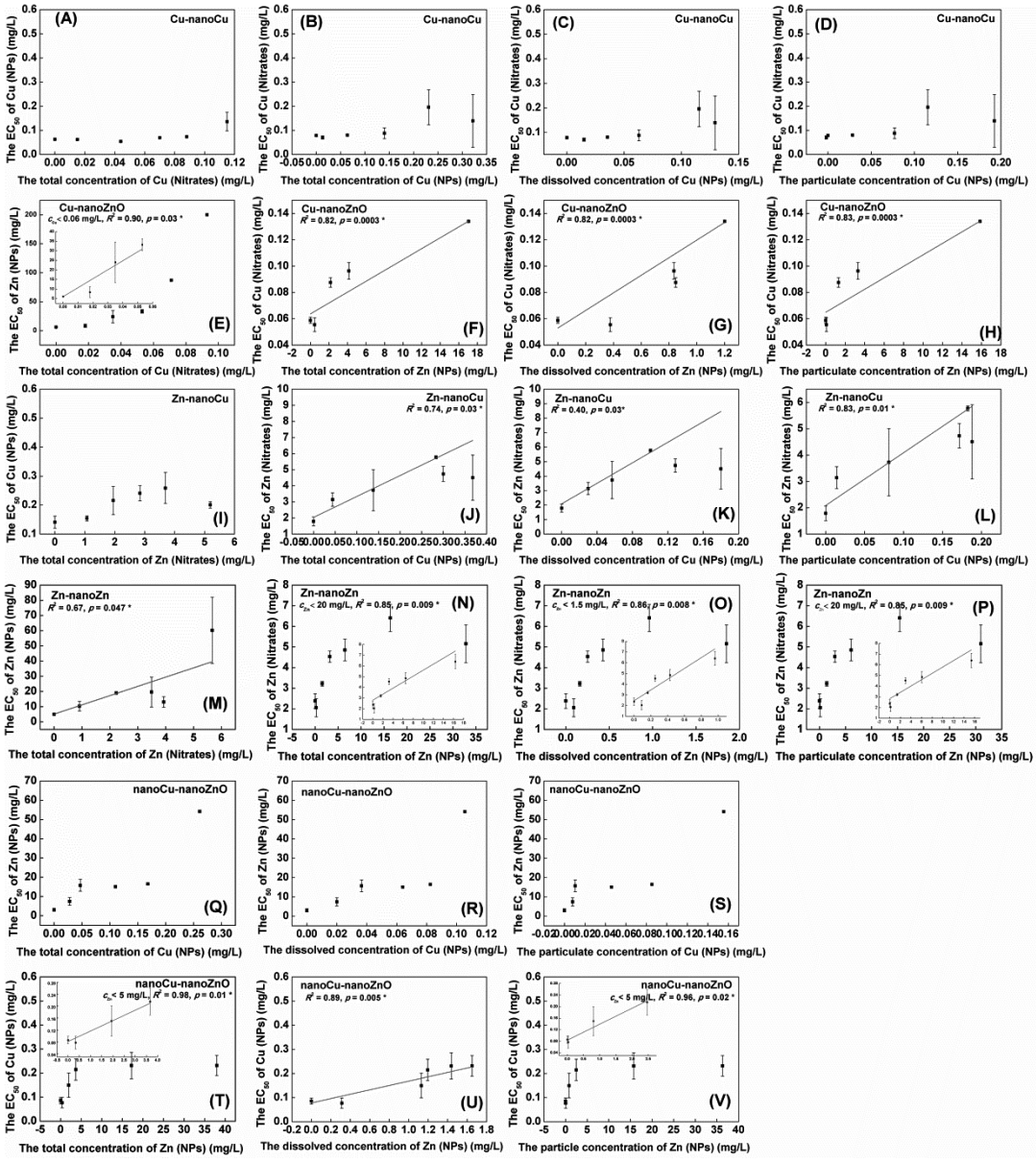

Figure 5.3 Relationships between the median effective concentrations (EC_{50}s) of $Cu(NO_3)_2$, $Zn(NO_3)_2$, Cu NPs, ZnO NPs for *L. sativa* L. after 4 d of exposure and the total concentration (or dissolved, or particulate concentration) of Cu NPs, ZnO NPs,

$Zn(NO_3)_2$, or $Cu(NO_3)_2$. Data are presented as mean ± standard error of the mean. Solid lines represent the statistically significant linear regression fits to figure out the overall synergistic or antagonistic effects. R^2 indicates the determination coefficient adjusted for the degrees of freedom. *p* indicates the statistical significance level. * indicates that the slope of linear curve is significantly different from zero at the 5% significance level.

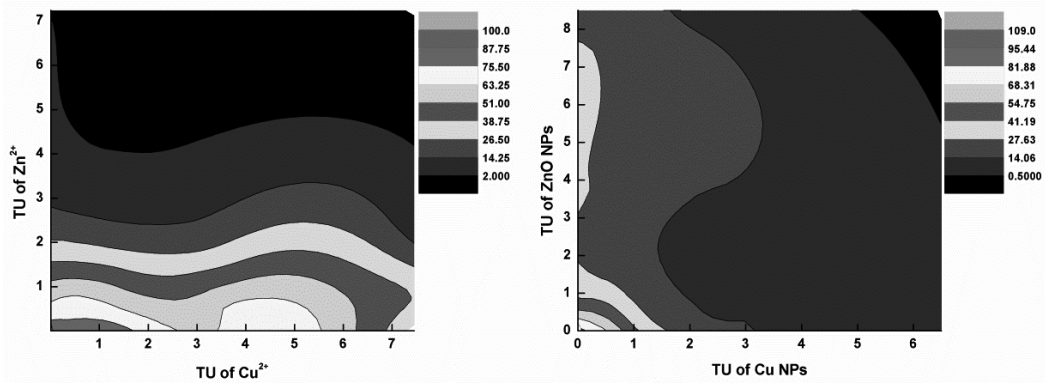

Figure 5.4 2D isobolic representation of the biological responses (*RRE*, %) for mixtures of $Cu(NO_3)_2$ and $Zn(NO_3)_2$ and mixtures of Cu NPs and ZnO NPs. The values of *RRE* are high in the negative control groups and decrease as doses of compounds increase. The x-axis or y-axis is presented as toxic unit (TU) for each compound (1TU=the value of median effective concentration which was shown in Table 5.1).

5.4.2 Toxicity of individual compounds

Our results showed that Cu is more toxic to lettuce seedlings than Zn regardless of the metal being in the form of a cation or a nanoparticle. This may be attributed to the different demands of plant cells for Cu and Zn in the growth and development. To our knowledge, similar studies were not conducted before, which made it difficult to compare the EC_{50} values of Cu NPs and ZnO NPs calculated in this study with those in other studies. Substantial differences in EC_{50}s can be caused by diverse properties of metal-based NPs e.g. size and shape, by different sensitivities of plant, and by different periods of plant growth.

5.4.3 Combined toxicity of Cu NPs and ZnO NPs

The good fitting provided by the standard IA model and the non-significant

'interactions' observed for Cu-nanoCu mixtures simultaneously verified the assumption of Song et al. (2014) that the addition model can be used to estimate the relative contribution of ionic and particulate forms to the cytotoxicity of Cu NPs. The IA model also showed a reasonable predictive power in estimating toxicity of Zn-nanoZnO mixtures and the rest of variations in modelling were explained by small antagonistic effects found in mixtures of Zn-nanoZnO. Since significant interactions were not observed on the dissolution and aggregation of ZnO NPs, the dissolved Zn may compete with the particulate Zn at the organism level, which influenced the toxicity of each other. Based on the antagonistic effects observed in mixtures of Cu-nanoZnO and Zn-nanoCu, it was suggested that the dissolved Zn may interact with the dissolved Cu which was consistent with the competition between Cu^{2+} and Zn^{2+} reported in previous studies of Le et al. (2013) and Liu et al. (2014). The feed-back mechanism (Qiu and Hogstrand, 2005) may be an explanation that an increase of copper in plant cell decreases the quantity of zinc importer proteins and blocks channels for zinc. In turn, the presence of low amounts of zinc may exert a positive effect on cell homeostasis and on the tolerance of cells to copper (Li et al., 2015). Until now, only Li et al. (2015) reported the potentiation effects on the human hepatoma cell line HepG2 co-exposed to Cu NPs and ZnO NPs and suggested that the nano-particulate fractions of ZnO NPs were attributable to the enhancement of Cu NPs toxicity. In contrast to the first finding of Li et al. (2015), antagonistic effects were observed in this study between Cu NPs and ZnO NPs on the toxicity of each other to lettuce. This may be caused by different features between animal cells and plant cells which lead to a diverse bioavailability or toxicity across species. In compliance with the second finding of Li et al. (2015), the particulate fractions of NPs were also observed to correlate with the 'interactions' and the overall toxicity of Cu NPs and ZnO NPs. This can be a reason that lead to a small deviation from 'additivity' in IA modeling and a difference in 2D isobolic representations between nanoCu-nanoZnO mixtures and mixtures of $Cu(NO_3)_2$ and $Zn(NO_3)_2$. The results of Zn-nanoCu, Cu-nanoZnO, Cu-nanoCu, and Zn-nanoZnO mixtures showed that the observed antagonistic effects between Cu NPs and ZnO NPs may be attributed to 'interactions' between dissolved Cu and dissolved Zn, between particulate Zn and dissolved Zn, of particulate Cu on dissolved Zn, and of particulate Zn on dissolved Cu at the organism level.

5.5 Conclusions

Our study first showed the commonly known independent action model can be used as a starting point to predict mixture effects of metal-based NPs. By dividing each type of metal-based NPs into a part of highly soluble metal species and a part of undissolved particles, we did record small antagonistic effects between these two parts of ZnO NPs which resulted in small deviations (16%) from 'additivity' in toxicity modelling. Similar effects were not observed for mixtures of Cu-nanoCu and therefore 94% variations in root growth could be explained by the IA model. The toxicity of ZnO NPs was found to be significantly decreased upon increasing concentrations of $Cu(NO_3)_2$ in solution, and vice versa. The EC_{50}s of $Zn(NO_3)_2$ were also highly correlated to the total (or dissolved, or particulate) concentrations of Cu NPs. Based on the above results, the small antagonistic effects observed between Cu NPs and ZnO NPs can be attributed to 'interactions' found among dissolved metal species as well as particulate fractions and lead to small deviations from 'additivity' (R^2=0.82), which cannot be easily explained by a simple combination of $Cu(NO_3)_2$ and $Zn(NO_3)_2$. To our knowledge, this is an innovative research in which data were generated on physic-chemical behavior as well as on biological effects of ZnO NPs, Cu NPs and their mixtures. Although the mechanism of interactions remains to be determined, there is no doubt that our research will enrich the rapid evolving field of nano-toxicology and help scientists develop approaches to evaluate the potential impacts of metal-based NPs and their mixtures on eco-systems.

Table 5.2 Interactions found between compounds in mixtures of Cu-Zn, Cu-nanoCu, Zn-nanoZnO, Cu-nanoZnO, Zn-nanoCu, and nanoCu-nanoZnO in the exposure of 4 d lettuce seedlings.

Compound 2 \ Compound 1	$Zn(NO_3)_2$	$Cu(NO_3)_2$	Cu NPs	Dissolved Cu	Particulate Cu
$Cu(NO_3)_2$	Anta\Anta (Le et al., 2013; Liu et al., 2014)	n.d.	No\No	No\n.d.	No\n.d.
$Zn(NO_3)_2$	n.d.	Anta\Anta (Le et al., 2013; Liu et al., 2014)	Anta\No	Anta\n.d.	Anta\n.d.
ZnO NPs	Anta\Anta	Anta\Anta	No\Anta	No\n.d.	No\n.d.
Dissolved Zn	n.d.\Anta	n.d.\Anta	n.d.\Anta	n.d.	n.d.
Particulate ZnO	n.d.\Anta	n.d.\Anta	n.d.\Anta	n.d.	n.d.

No significant effect (No): the slope of linear fits in Figure 5.3 is not significantly different from zero which indicates that no significant effects of one component observed on the EC_{50}s of other components in the mixture; Antagonism (Anta): the slope of linear fits in Figure 5.3 significantly deviates from zero with increasing concentrations of one mixture component which indicates an antagonistic effect of one compound on another compound in the mixture; n.d.: not determined in this study; \: the left side indicates the impacts of Compound 1 on Compound 2 and the right side indicates the impacts of Compound 2 on Compound 1.

References

Adamson AW, Gast AP. 1997. Physical chemistry of surfaces. New York, United States: Wiley.
Batley GE, Kirby JK, McLaughlin MJ. 2012. Fate and risks of nanomaterials in aquatic and terrestrial environments. Accounts Chem Res 46, 854-862.
Blinova I, Ivask A, Heinlaan M, et al. 2010. Ecotoxicity of nanoparticles of CuO and ZnO in natural water. Environ Pollut 158, 41-47.
Bliss CI. 1939. The toxicity of poisons applied jointly. Ann Appl Biol 26, 585-615.
Bolyard SC, Reinhart DR, Santra S. 2013. Behavior of engineered nanoparticles in landfill leachate. Environ Sci Technol 47, 8114-8122.
Bondarenko O, Ivask A, Käkinen A, et al. 2012. Sub-toxic effects of CuO nanoparticles on bacteria: Kinetics, role of Cu ions and possible mechanisms of action. Environ Pollut 169, 81-89.
Bongers M. 2007. Mixture toxicity of metals to Folsomia candida related to (bio)availability in soil. Ph.D. Thesis, Vrije Universiteit Amsterdam, The Netherlands.
Borm P, Klaessig FC, Landry TD, et al. 2006. Research strategies for safety evaluation of nanomaterials, part V: role of dissolution in biological fate and effects of nanoscale particles. Toxicol Sci 90, 23-32.
Bystrzejewska-Piotrowska G, Golimowski J, Urban PL. 2009. Nanoparticles: their potential toxicity, waste and environmental management. Waste Manage 29, 2587-2595.
Cedergreen N, Sørensen H, Svendsen C. 2012. Can the joint effect of ternary mixtures be predicted from binary mixture toxicity results? Sci Total Environ 427, 229-237.
EPA. 1988. Protocols for short term toxicity screening of hazardous waste sites; EPA 600/3-88/029: Washington DC, U.S.
Fernández-Cruz ML, Lammel T, Connolly M, et al. 2013. Comparative cytotoxicity induced by bulk and nanoparticulated ZnO in the fish and human hepatoma cell lines PLHC-1 and Hep G2. Nanotoxicology 7, 935-952.
Franklin NM, Rogers NJ, Apte SC, et al. 2007. Comparative toxicity of nanoparticulate ZnO, bulk ZnO, and $ZnCl_2$ to a freshwater microalga (Pseudokirchneriella subcapitata): the importance of particle solubility. Environ Sci Technol 41, 8484-8490.
Holsapple MP, Farland WH, Landry TD, et al. 2005. Research strategies for safety evaluation of nanomaterials, part II: toxicological and safety evaluation of nanomaterials, current challenges and data needs. Toxicol Sci 88, 12-17.
Hu CW, Li M, Cui YB, et al. 2010. Toxicological effects of TiO_2 and ZnO nanoparticles in soil on earthworm *Eisenia fetida*. Soil Biol Biochem 42, 586-591.
Ivask A, Juganson K, Bondarenko O, et al. 2013. Mechanisms of toxic action of Ag, ZnO and CuO nanoparticles to selected ecotoxicological test organisms and mammalian cells in vitro: A comparative review. Nanotoxicology 8, 57-71.
Kahru A, Dubourguier HC. 2010. From ecotoxicology to nanoecotoxicology. Toxicology 269, 105-119.
Karlsson HL, Gliga AR, Calléja FM, et al. 2014. Mechanism-based genotoxicity screening of metal oxide nanoparticles using the ToxTracker panel of reporter cell lines. Part Fibre Toxicol 11, 1-14.
Le TTY, Vijver MG, Hendriks AJ, et al. 2013. Modeling toxicity of binary metal

mixtures (Cu^{2+}-Ag^{+}, Cu^{2}+-Zn^{2+}) to lettuce, *Lactuca sativa*, with the biotic ligand model. Environ Toxicol Chem 32, 137-143.
Li M, Lin D, Zhu L. 2013. Effects of water chemistry on the dissolution of ZnO nanoparticles and their toxicity to Escherichia coli. Environ Pollut 173, 97-102.
Li L, Fernández-Cruz ML, Connolly M, et al. 2015. The potentiation effect makes the difference: Non-toxic concentrations of ZnO nanoparticles enhance Cu nanoparticle toxicity in vitro. Sci Total Environ 505, 253-260.
Liu Y, Vijver MG, Peijnenburg WJGM. 2014. Comparing three approaches in extending biotic ligand models to predict the toxicity of binary metal mixtures (Cu–Ni, Cu–Zn and Cu–Ag) to lettuce (*Lactuca sativa* L.). Chemosphere 112, 282-288.
Misra SK, Dybowska A, Berhanu D, et al. 2012. The complexity of nanoparticle dissolution and its importance in nanotoxicological studies. Sci Total Environ 438, 225-232.
Mortimer M, Kasemets K, Kahru A. 2010. Toxicity of ZnO and CuO nanoparticles to ciliated protozoa *Tetrahymena thermophila*. Toxicology 269, 182-189.
OECD. 2006. OECD Test Guidelines 208: Terrestrial plant test-seedlings emergence and seedling growth test. OECD Guidelines for the Testing of Chemicals, Paris.
Pfleeger T, Mc Farlane C, Sherman R, et al. 1991. Short-term bioassay for whole plant toxicity. In: Gorsuch JW (Ed.), Plants for toxicity assessment. ASTM Special Technical Publication, Ann Arbor, pp. 355-364.
Qiu A, Hogstrand C. 2005. Functional expression of a low-affinity zinc uptake transporter (FrZIP2) from pufferfish (Takifugu rubripes) in MDCK cells. Biochem J 390, 777-786.
Rico CM, Majumdar S, Duarte-Gardea M, et al. 2011. Interaction of nanoparticles with edible plants and their possible implications in the food chain. J Agr Food Chem 59, 3485-3498.
Rousk J, Ackermann K, Curling SF, et al. 2012. Comparative toxicity of nanoparticulate CuO and ZnO to soil bacterial communities. PloS one 7, e34197.
Song W, Zhang J, Guo J, et al. 2010. Role of the dissolved zinc ion and reactive oxygen species in cytotoxicity of ZnO nanoparticles. Toxicol Lett 199, 389-397.
Song L, Connolly M, Fernández-Cruz ML, et al. 2014. Species-specific toxicity of copper nanoparticles among mammalian and piscine cell lines. Nanotoxicology 8, 383-393.

Supplementary Materials

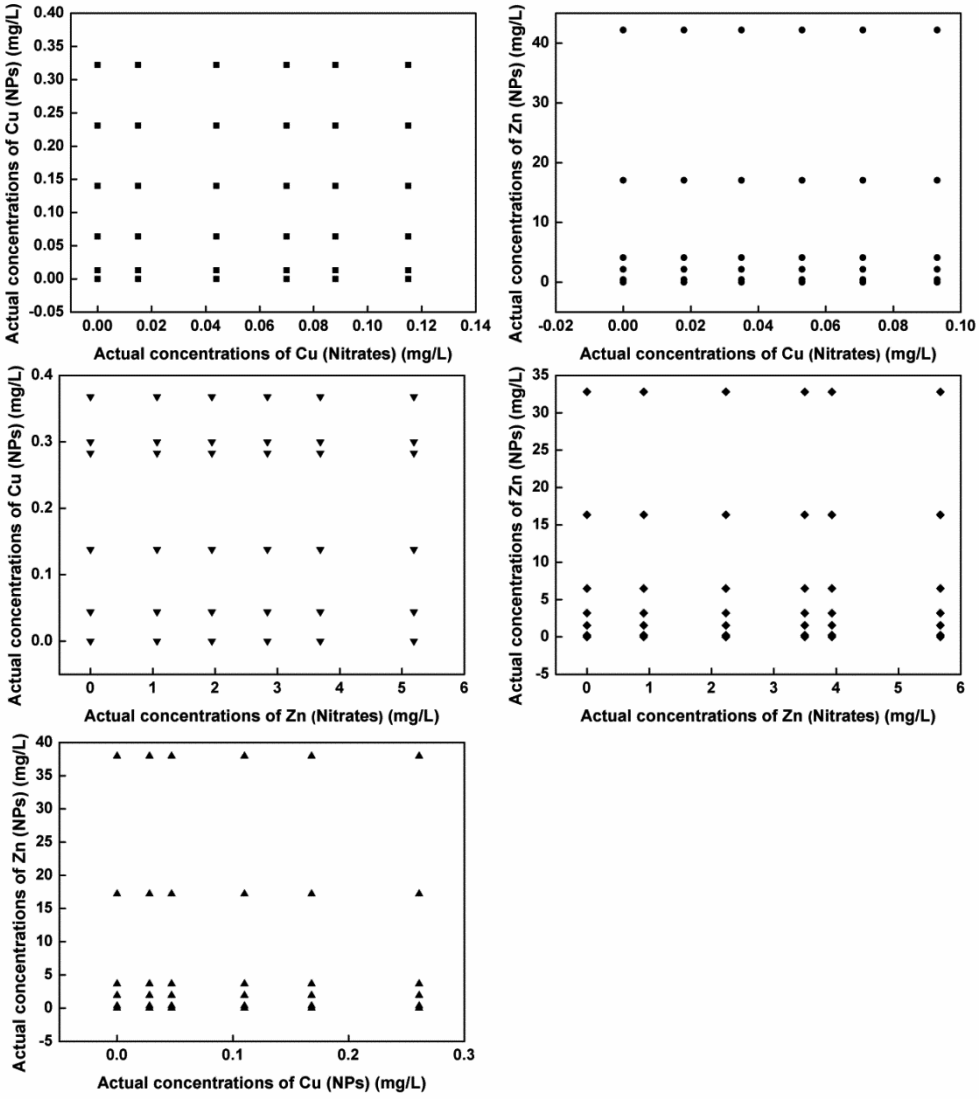

Figure S5.1 The set-up for Cu-nanoCu, Cu-nanoZnO, Zn-nanoCu, Zn-nanoZnO, and nanoCu-nanoZnO mixtures expressed as actual concentrations tested by the Flame AAS.

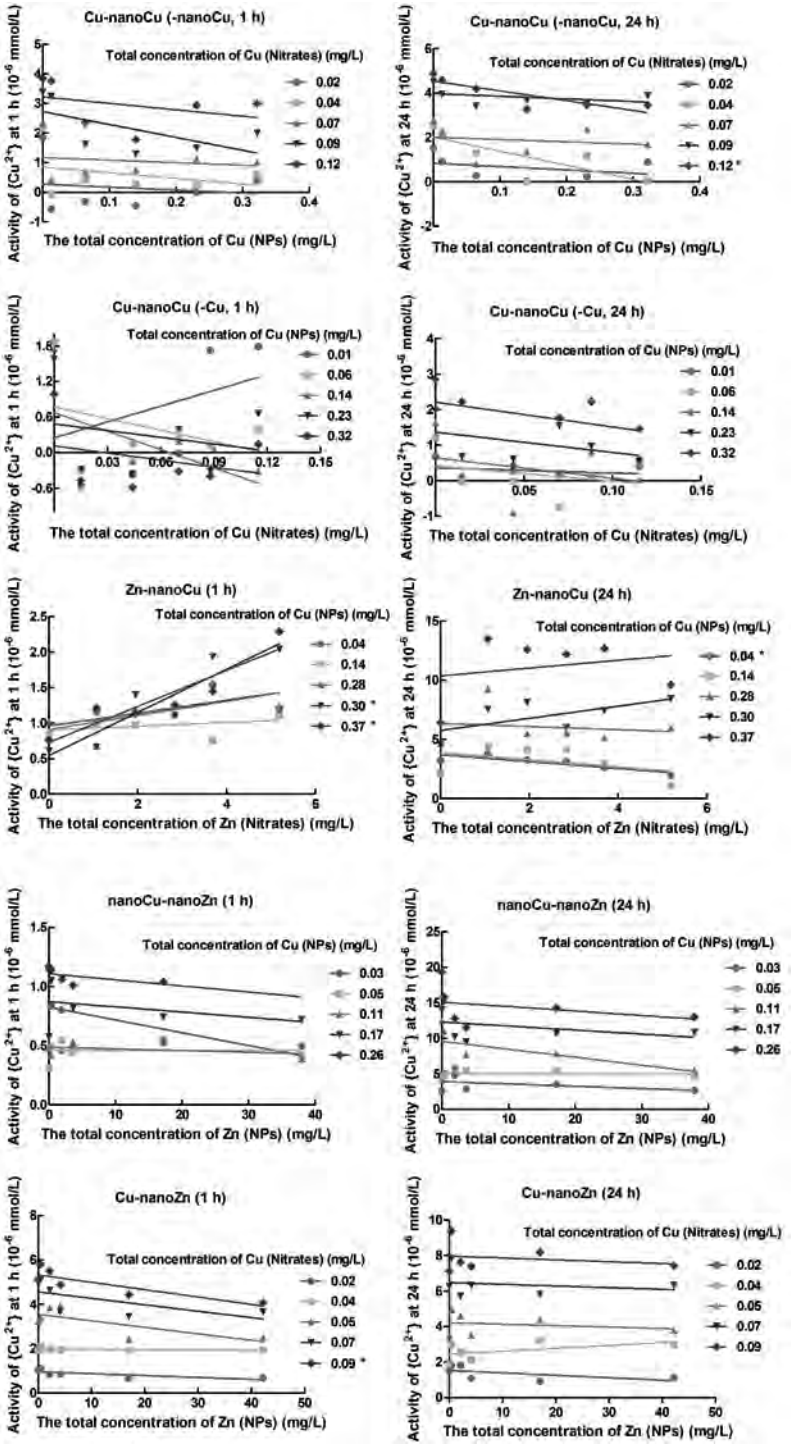

Figure S5.2 Relationships between free Cu^{2+} activities in the solution and the added

amount of ZnO NPs, $Zn(NO_3)_2$, Cu NPs, $Cu(NO_3)_2$ after 1 h and 24 h of equilibration. For the combination of Cu-nanoCu, the activities of Cu^{2+} released from Cu NPs equal to the total Cu^{2+} activities minus the activities of Cu^{2+} released from $Cu(NO_3)_2$, and vice versa. The solid lines represent linear relationships. * indicates that the slope of linear curve is significantly different from zero at the 5% significance level. {} indicates the free ion activities.

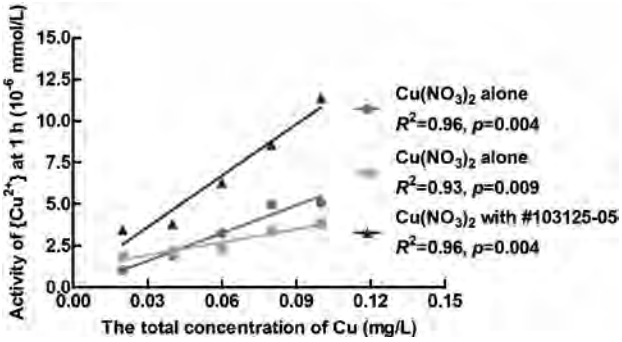

Figure S5.3 Relationships between free Cu^{2+} activities in solution and the added amount of $Cu(NO_3)_2$ in the presence of plain polystyrene fluorescent microspheres after 1 h of equilibration. The total concentration of Cu is the mean value (n=2) of actual concentration of Cu in nitrate salts measured by FAAS. #103125-05 indicates the plain polystyrene fluorescent microspheres. The solid lines represent linear relationships. R^2 indicates coefficient of determination. p indicates the statistical significance level.

Table S5.1 Particle characterization of nano-Cu, nano-ZnO and five mixtures expressed as mean ± standard error of the mean (SEM) by dynamic light scattering.

Compounds	Size distribution (nm)		Zeta-potential (mV)	
	1 h	24 h	1 h	24 h
Nano-Cu	370 ± 36	786 ± 107	-12.7 ± 0.4	-5.5 ± 0.4
Nano-ZnO	1016 ± 28	1487 ± 33	0.9 ± 0.1	-6.5 ± 0.3
Cu-nanoCu	851 ± 26	815 ± 26	-13.6 ± 0.7	-9.2 ± 0.6
Zn-nanoCu	418 ± 32	631 ± 58	-11.4 ± 0.6	-4.4 ± 0.4
NanoCu-nanoZnO	644 ± 37	1531 ± 101	-8.5 ± 0.5	-10.8 ± 0.4
Cu-nanoZnO	1060 ± 90	1010 ± 144	-5.6 ± 0.3	-4.1 ± 0.3
Zn-nanoZnO	1222 ± 166	1365 ± 93	8.1 ± 0.9	-7.3 ± 0.6

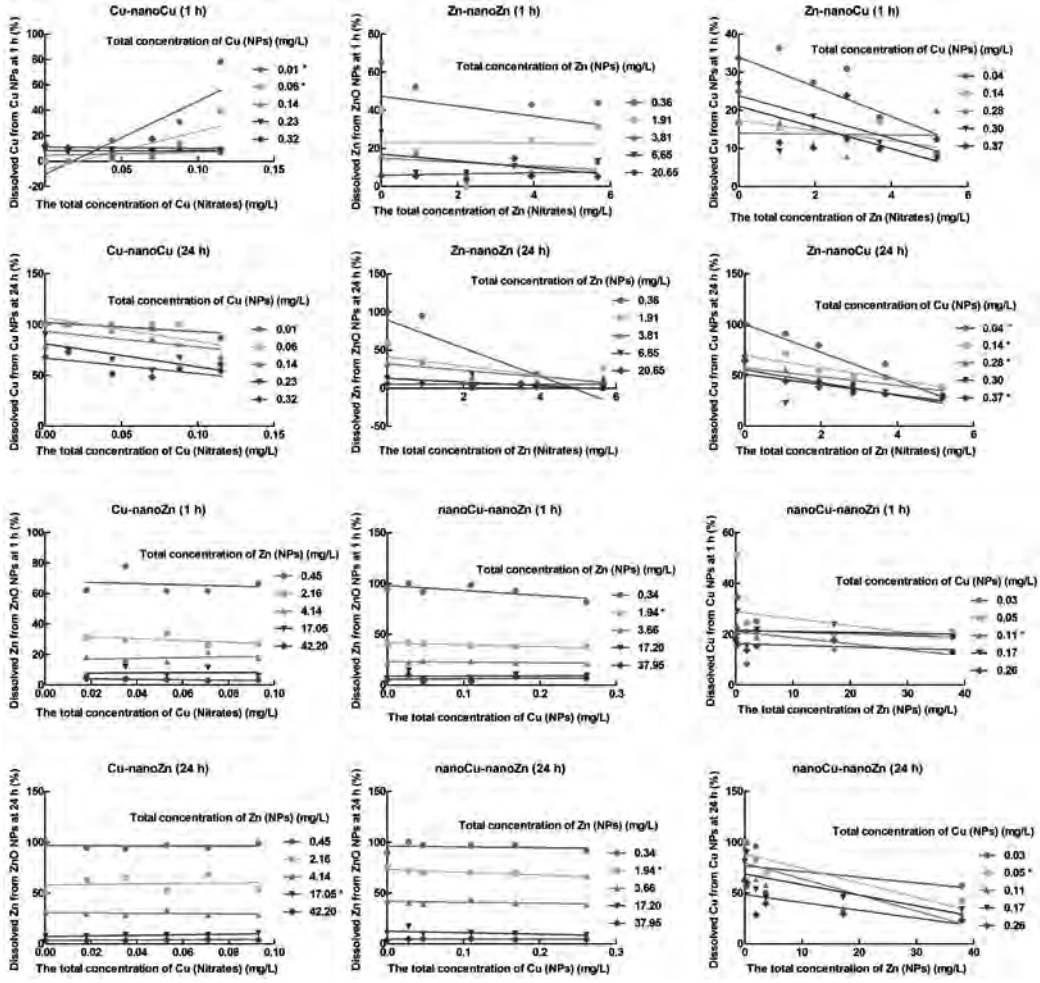

Figure S5.4 Relationships between the percentage of dissolved concentrations divided by the total concentrations of one compound and the added amount of other compounds in mixtures of Cu-nanoCu, Zn-nanoZnO, Cu-nanoZnO, Zn-nanoCu, nanoCu-nanoZnO after 1 h and 24 h of equilibration. The solid lines represent linear relationships. * indicates that the slope of linear curve is significantly different from zero at the 5% significance level.